

Impact of precipitation intensity and drought patterns on groundwater storage fluctuations within the Ghis-Nekor aquifer (Morocco)

Taoufik Ahalli¹ , Hasan Ouakhir^{2*} , Nordine Nouyati^{1*} , Driss Khattach³ ,
Nadia Ennaji⁴ , Mimoun Goumih⁵ , Aziz Maziane² , Anass Aynaou¹ ,
Fatima Zahra Talbi⁶ 

¹ Environmental Management and Civil Engineering Team, Applied Sciences Laboratory, National School of Applied Sciences, Abdelmalek Essaadi University, Al Hoceima, 32002, Morocco

² Higher Institutes of Nursing and Health Technology Professions, Demography and Environment, Beni Mellal, Morocco

³ Applied Geosciences Laboratory, Faculty of Sciences, University Mohammed Premier, Oujda 60000, Morocco

⁴ Sidi Mohamed Ben Abdellah University, Faculty of Polydisciplinary, Laboratory of Space, History, Dynamic and Development; Physical geography; 35000 Taza, Morocco

⁵ Laboratory Dynamic of Landscape, Risk and Heritage, Sultan Moulay Slimane University, Béni Mellal, Morocco

⁶ Sidi Mohamed Ben Abdellah University, Faculty of Sciences Dhar El Mahraz, Laboratory of Biotechnology Conservation and Valorization of Natural Resources, 30000 Fez, Morocco

* Corresponding author's e-mail: nnouayti@uae.ac.ma, h.ouakhir@usms.ma

ABSTRACT

The present study examines the influence of precipitation intensity, and drought patterns on groundwater levels within the Ghis-Nekor aquifer, which is located in an arid and semi-arid region of Morocco. Besides, by using satellite-derived datasets and the innovative trend analysis (ITA) method, the research analyzed the trends in groundwater storage (GWS), which offers a more robust approach to detect long-term changes compared to traditional methods, such as the Mann-Kendall test. The study used the gravity recovery and climate experiment (GRACE), gridded data to estimate groundwater fluctuations, the assess the time-series trends in equivalent water thickness (EWT), and soil moisture. The obtained results indicate a significant decline in groundwater levels, with 40% of monitoring sites, which showed a substantial downward trend, and 60% experiencing even more pronounced decreases. Furthermore, the maximum estimated groundwater storage loss is 2.4 cm/year¹. These findings underline the detrimental effects of overexploitation and inefficient irrigation practices, which contribute to ecological degradation, including increased salinity, and groundwater pollution. Although the reliance of the study on satellite data offers valuable insights, it may overlook localized variations, and the GRACE data may be less accurate in the areas with complex geological features. Despite these limitations, the research provides practical value by informing water management strategies aimed to mitigate groundwater depletion. Consequently, the novelty of this study lies in the use of the ITA technique to correlate and improve trend detection accuracy, which offer a more comprehensive understanding of groundwater changes, and support a sustainable water management practice in vulnerable areas like Ghis Nekor basin.

Keywords: groundwater level, precipitation intensity, drought patterns, Ghis-Nekor aquifer, innovative trend analysis, water management

INTRODUCTION

Climatic projections predict a substantial increase in temperature, accompanied by a drop in annual rainfall and a probable escalation of extreme

rainfall events in several regions of the Mediterranean basin (Ouakhir et al., 2023a). Consequently, susceptibility to these catastrophic food shortages and drought disasters may escalate, particularly in developing nations (Salhi et al., 2019).

In this context, water resource management, especially groundwater, is critical in arid and semi-arid regions like northern Morocco, where water scarcity is exacerbated by climate variability and human activities (Ennaji et al., 2022). The Ghis-Nekor aquifer is a crucial water source in this area, yet groundwater levels have been impacted by both climate change and over-exploitation (Ennaji et al., 2024).

Recent advancements in satellite-based climate data, such as those from the Gravity Recovery and Climate Experiment (GRACE), have proven effective in studying groundwater fluctuations and water storage dynamics (Chakir et al., 2024). While many studies have successfully applied satellite data to hydrological assessments, the integration of such data for specific aquifers, like Ghis-Nekor, remains underexplored. This study aimed to bridge this gap by evaluating the contribution of GRACE satellite data in understanding groundwater changes in the Ghis-Nekor aquifer, alongside traditional in situ measurements.

The main objective of this paper was to assess the impacts of precipitation and drought on groundwater fluctuations. Furthermore, the study focused on the identification of new patterns, and trends in groundwater storage using advanced methods like the innovative trend analysis (ITA) (Güçlü, 2018). Besides, based on the exploring of these relationships, the study will contribute valuable insights for water resource management, bridging a critical gap in the scientific understanding of groundwater dynamics in the semi-arid regions like Morocco.

In summary, this study aimed to enhance the knowledge of the role of satellite climate data in hydrological studies, refine analytical techniques, and provide new insights into the effects of precipitation variability on groundwater storage, with implications for sustainable water management (Chen et al. 2019; Chen et al., 2022; Hamdi 2023a and b; Amraoui et al., 2024; Amraoui et al., 2023).

PRESENTATION OF STUDY AREA

Geographical location

The Ghis-Nekor plain is located within the Rif region of northern Morocco, approximately 12 km southeast of the coastal city of Al Hoceima. It occupies an area of about 100 km², and situated between both provinces of Al Hoceima, and Nador. The research area is linked to the national road network through National Road number 2, which connects Tangier to Oujda; however, with several curves and limited width, rendering it problematic. The linkage between the cities of Al Hoceima and Ajdir is facilitated by the primary route number 39.

Geographically, the plain is surrounded by rugged terrain, with the Mediterranean Sea to the north and steep mountainous regions to the south and east. The plain is characterized by a generally gentle slope of about 1% from south to the north, whereas its landscape features a mix of impermeable schist-sandstone flysch and

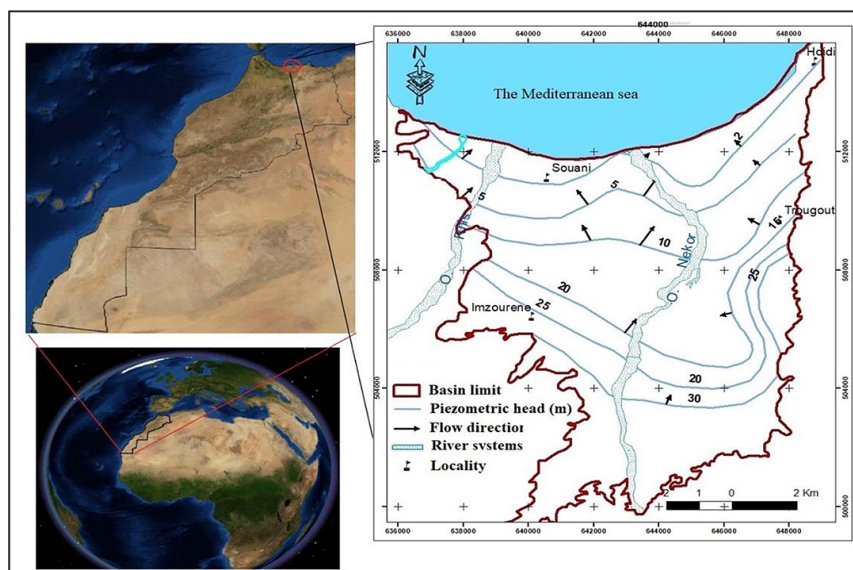


Figure 1 . Localization of the Ghis-Nekor basin, and the spatial distribution of sampling points

limestone ridges (Fig. 1) (Ouakhir et al., 2023). The area is intersected by the Ghis and Nekor rivers, which contribute to the hydrological dynamics of the area. Its location, combined with its geological and hydrological characteristics, makes the Ghis-Nekor plain a crucial area for studying groundwater fluctuations, particularly under the pressures of climate variability and human activity.

Geology

The Ghis-Nekor plain is an intra-mountainous valley characterized by a diverse alluvial deposit comprising sands, gravels, and conglomerates from the Plio-Quaternary period to the present. This depression stands around one hundred square km, and is predominantly encircled by impermeable schist-sandstone formations, with carbonate structures of the limestone ridge of the Bokoya massif to the northwest and Plio-Quaternary volcanic rocks of Ras Tarf to the northeast (Klemme, 1958). Besides, the eastern border manifests as a piedmont characterized by a juxtaposition of alluvial fans, the most prominent of which is situated in the southeast. Moreover, the assessment of the Physicochemical Water Quality of the Ghis-Nekor Aquifer (Al Hoceima, Morocco) is made by Utilizing Hydrochemistry, Multiple Isotopic Tracers, and Geographic Information System (GIS).

Hydrogeological characteristics

The Ghis-Nekor plain is traversed by two perennial rivers, the Rhis and Nekor Rivers, with the latter receiving seasonal tributaries, the Amekrane and Tifarouine rivers, during flood periods. The Nekor river has a watershed of 911 km², with an average altitude of 1008 m a.s.l, and flows for 69 km at a 2.4% average slope (Nouayti et al., 2022). Furthermore, the aquifer in this area consists of coarse alluvium with varying thickness, from 64 m in the southern basin to over 400 m in the central basin. It is composed of sandy-gravel alluvium, limonite layers, and clayey-marly lenses (Chakir et al., 2023). The hydrodynamic characteristics of the aquifer reveal a transmissivity range of 10^{-4} to 6.4×10^{-2} , a storage coefficient between 0.65×10^{-2} and 5.3×10^{-2} , and groundwater productivity exceeding 100 l/s, with flow moving from south to north.

DATA, METHODS AND TECHNIQUES

Satellite data

Climate and TWS data are readily available and accessible for download from NASA and other websites, where monthly measurement files can be obtained. A Python application has been developed to extract and visualize these datasets in the form of maps or time series. In this study, *GRACE* and *GRACE-FO TWS* data were downloaded from the Table 1, within *NetCDF* format (*CSR_GRACE_GRACE-FO_RL0602_Mascons_all-corrections.nc*), covering the period from April 2002 to March 2024 (last updated on: 2024-06-18). The data is represented on a 1/4 degree longitudinal-lateral grid, but corresponds to a 1×1 degree equal-area geodetic grid at the equator, which is the current native resolution for *CSR RL06* mascon solutions. This new *RL06* grid, with a 1/4-degree resolution (compared to 1/2 degree in *RL05*), was designed to more accurately represent coastlines. The final dataset includes monthly *TWS* anomalies in centimeters (cm) of equivalent water thickness from April 2002 to February 2023. Missing *GRACE* observations were interpolated linearly, using the values from the two adjacent months.

The method of chronological decomposition of precipitation data series

The decomposition method is an approach used in signal processing, and image processing to decompose a signal or image into components that can be fine details or important structures. A time series can be broken down into three elements (Fig. 2).

- The trend represents the long-term evolution of the series studied: it reflects the “average” behavior of the series (observed).

Table 1. Data source and availability

SPI or SSFI values	Degree of humidity or dryness
>+2.0	Extreme humidity
+1.5 to +1.99	High humidity
+0.1 to +1.49	Low humidity
+0.1 to +0.99	Light humidity
0	Absolute normality
-0.1 to -0.99	Mild drought
-1.0 to -1.49	Moderate drought
-1.5 to -1.99	Severe drought
<-2.0	Extreme drought

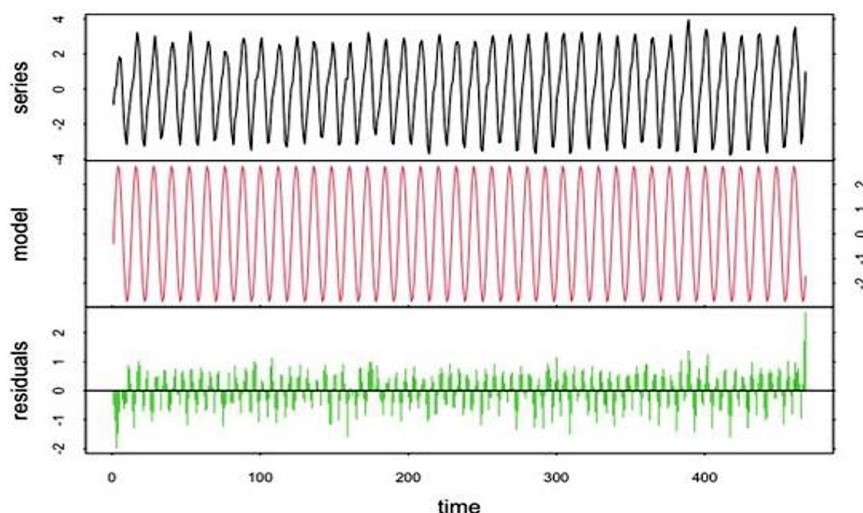


Figure 2. Example of chronological decomposition of a precipitation series

- The seasonal component or seasonality (seasonal) corresponds to a phenomenon that repeats itself at regular time intervals (periodic). In general, it is a seasonal phenomenon, hence the term seasonal variations.
- The residual component or noise or residue (*random*): these are irregular fluctuations of a random nature. It is obtained by removing the trend and seasonal movements from the initial series. In addition, graphs of this study were drawn from NASA data.

(1948) derived the statistical distribution of the test (Drouiche *et al.*, 2019). This test is suitable for cases where the trend can be assumed to be monotonic and therefore no seasonal aspect is presented in the data. A major advantage of the Mann-Kendall test is that: it is not a presupposition method in terms of data distribution, i.e., there are no assumptions needed about the data distribution as the prerequisite for this method is known as a non-parametric method (Drouiche *et al.*, 2019).

Mann-Kendall test

The Mann–Kendall (MK) statistic is a non-parametric test used for trend analysis. Mann (1945) was the first one to use this test, and Kendall

Innovative trend test

The simple ITA methodology provides insight into trend analysis, as it describes monotonic or non-monotonic increasing or decreasing trends (Fig. 3). Furthermore, considering five trend

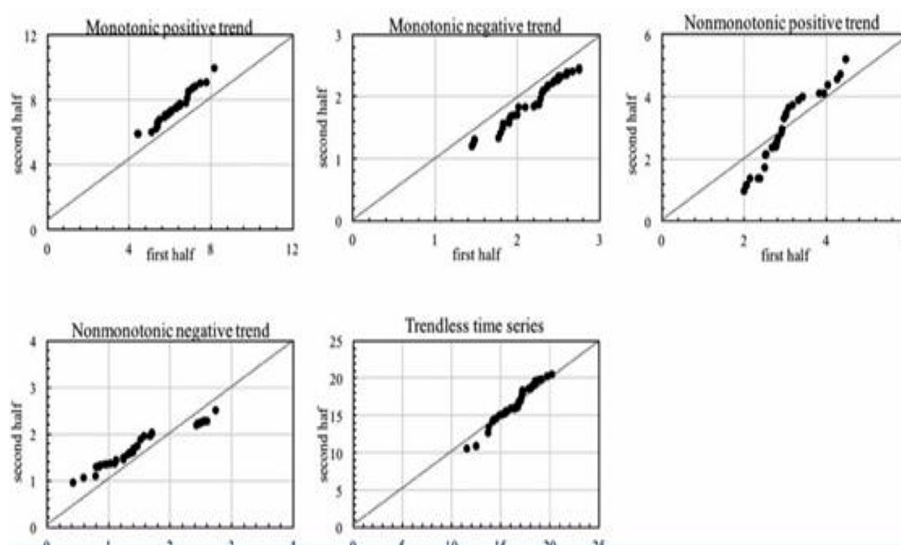


Figure 3. Example of the innovative trend ITA test

conditions: monotonic and non-monotonic decreasing, monotonic and non-monotonic increasing and no-trend type (Alifujiang *et al.* 2023). The basic procedure of ITA by dividing the observation data from the first data values to the final data values into two equal parts and sorting the two sub-data series in ascending order, respectively. On the basis of the on two-dimensional Cartesian coordinates, the first half of the data value (X_i) is located on the horizontal axis (X-axis), and the second half of the data value (X_j) is located on the vertical axis (O-axis). The span of both axes should be equal. The line (45°) divides the diagram into two similar triangles. If the data points accumulate on the 45° line, it is found that there is a time series without a trend.

If all data points lie above (below) the 45° line in the upper (lower) triangle area, there is a monotonic upward (downward) trend present in the time series data. Suppose the data points are nonlinearly accumulated above (below) the 45° line in the upper (lower) triangle area. In this case, the time series data exhibits a non-monotonic upward (downward) trend. The ITA method cannot display the number of time series and subcategories. However, the new innovative trend test analysis, as a new type of Şen methodology, indicates the mentioned trends and describes the number of data and subcategories (Alifujiang *et al.* 2023).

Standardized precipitation index

Table 2 shows the value of drought indices as a function of the degree of humidity or dryness. Droughts that impact water availability,

agricultural production and livestock operations are typically identified and characterized using drought indices. This study investigated the potential of using the standardized precipitation index (SPI) and the precipitation-based standardized precipitation- evapotranspiration index (SPEI) to reproduce the observed meteorological droughts at the Ghis-Nekor aquifer level.

The TWS data analysis method

To calculate terrestrial water storage anomalies, the following equation was used (Pascal., 2022):

$$TWS = SW + SM + GWS + SWE \quad (1)$$

where: SW – surface water, SM – soil moisture, GWS – groundwater, SWE – snow water equivalent.

As well as:

$$GWS = TWS - SM \quad (2)$$

RESULTS AND DISCUSSION

Climate context

The average precipitation reveals clear seasonal patterns with notable peaks in rainfall during the winter months and significant drops in the summer (Fig. 4). December records the highest average precipitation, exceeding 50 mm, followed closely by November, January, February, and March, all of which show substantial rainfall levels (40–50 mm). These peaks align with the winter season, which

Table 2. SPI values as a function of humidity or dryness

Month	p -value	Z	H0: No trend	Breast slope	Trend direction
January	0.7355	0.33782	Yes	0.1925926	No trend
February	0.7074	0.3754	Yes	0.1428571	No trend
March	0.0716	1.8011	Yes	0.9482143	No trend
April	0.0367	2.0883	No	0.8322917	Increase
May	0.6252	-0.48854	Yes	-0.0626087	No trend
June	0.1943	-1.2981	Yes	0	No trend
July	0.9599	-0.050247	Yes	0	No trend
August	0.1643	-1.3909	Yes	0	No trend
September	0.7639	0.30032	Yes	0.06333333	No trend
October	0.5609	-0.5815	Yes	-0.3818783	No trend
November	0.7497	0.319	Yes	0.2002262	No trend
December	0.4305	-0.78835	Yes	-0.4833333	No trend
Annual	0.1108	-1.5944	Yes	-2.163352	No tension

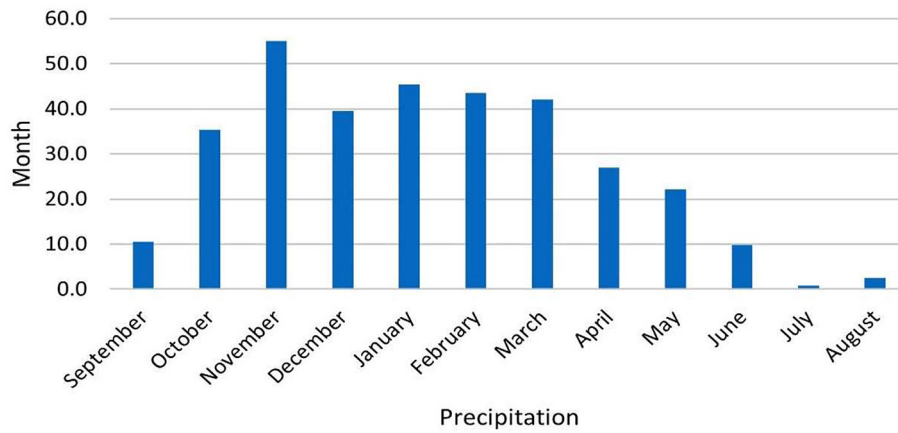


Figure 4 . Average monthly precipitation of the Ghis-Nekor aquifer

typically brings the wettest months in semi-arid Mediterranean regions, like Ghis-Nekor.

In contrast, the summer months (June to August) experience minimal rainfall, with July and August recording close to zero precipitation. This period highlights the dry season, exacerbating water scarcity and reducing groundwater recharge. Transitional months like April and May show a gradual decline in precipitation, reflecting the shift from winter to summer.

When analyzed alongside historical rainfall trends (e.g., 450 mm in 2005, 150 mm in 2015, and moderate levels of 300–320 mm in 2010 and 2018), the seasonal variability seen in this figure emphasizes the vulnerability of the Ghis-Nekor aquifer to drought and climate fluctuations. Prolonged low rainfall periods, such as in the summer, can further stress groundwater resources, necessitating effective water management strategies to address the recharge deficits during drought years (Ouakhir and El Ghachi, 2023).

Chronological decomposition of precipitation in the Ghis-Nekor plain

The decomposition of the monthly precipitation time series shown in Figure 5 highlights the key components of the variability in rainfall patterns over the observed period (2002–2021). The analysis separates the data into three main components: trend, seasonality, and residuals.

- Original data (top panel) – the original precipitation series shows significant variability with multiple peaks and troughs across the years. Higher precipitation events are visible between 2008–2010 and again around 2018–2019, which indicate periods of increased rainfall intensity. The fluctuations emphasize the irregular nature of rainfall in the study area.
- Trend (second panel) – the trend component reveals long-term variations in rainfall. There is a noticeable decline in rainfall

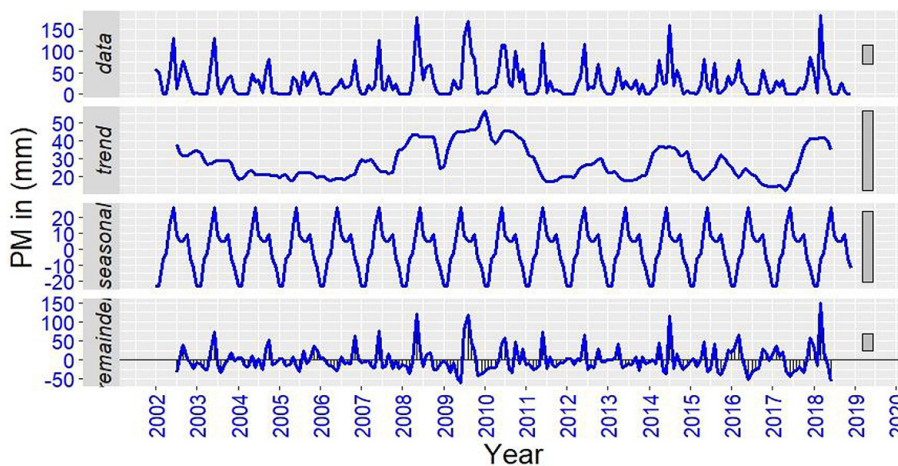


Figure 5. Decomposition of the precipitation data series in the Ghis-Nekor plain during 1992–2021

between 2002 and 2008, followed by a slight recovery and stabilization during 2010–2015. From 2016 onward, the trend shows another upward movement, and showed an increase of precipitation levels in recent years. This trend analysis reflects the periods of drought and recovery, consistent with broader climate variability patterns.

- Seasonality (third panel) – the seasonal component highlights a consistent annual cycle in precipitation. Peaks occur during the winter months, reflecting the Mediterranean climate of the Ghis-Nekor area, where rainfall is concentrated in winter. This seasonal pattern remains steady throughout the observed period, underscoring the regular occurrence of wet and dry seasons.
- Residuals (bottom panel) – the residuals represent the irregular or random variations not captured by the trend and seasonal components. These fluctuations are more prominent in the years with extreme rainfall anomalies, such as 2008 and 2019. This highlights the events that deviate from typical patterns, likely caused by short-term climatic factors or localized weather phenomena.

In summary, the time series decomposition effectively isolates the underlying components of precipitation variability. The seasonality is stable, driven by annual climatic cycles, while the trend indicates periods of drought and recovery. The residuals show irregular fluctuations that may signal extreme weather events, emphasizing the need for adaptive water resource management in response to climatic variability.

Innovative trend test to analyze temporal dynamics at the Ghis-Nekor aquifer level

The results of the Mann-Kendall test for monthly precipitation trends at the Ghis-Nekor station between 1992 and 2020 are presented in Table 3. The analysis reveals that April is the only month showing a significant upward trend in precipitation, with a p-value of 0.0367 (less than the 0.05 significance threshold) and a positive Z-value (2.0883). This indicates a statistically significant increase in rainfall during April, as confirmed by the positive Sen’s slope value (0.8323).

For the other months, no significant trends were observed. The p-values for all months, except April, are greater than 0.05, and the Z-values hover around zero, indicating no monotonic trend in precipitation. For instance, January (p-value: 0.7355) and February (p-value: 0.7074) show no trend, while months like May and October exhibit negative Z-values, though they remain statistically insignificant. The annual trend, with a p-value of 0.1108 and a Z-value of -1.5944, does not indicate any significant long-term variation in precipitation either.

Overall, the results suggest that April is experiencing an upward trend in rainfall, which could potentially contribute to groundwater recharge during this month. However, the lack of significant trends in other months highlights the high variability and inconsistency of precipitation patterns over the years. This aligns with the observed effects of drought and climate variability, which continue to impact groundwater resources in the Ghis-Nekor basin, emphasizing the vulnerability of the region’s water table to climate change.

Table 3. Results of the Man-Kendall test at the Ghis-Nekor water table during 1992–2021

Month	Low (<20 mm)	Average (20–40 mm)	Strong (>40 mm)
January	Yes (+)	Yes (+)	Yes (+)
February	Yes (+)	Yes (+)	Yes (+)
March	Yes (-)	Yes (-)	Yes (-)
April	Yes (+)	Yes (+)	Yes (+)
May	Yes (+)	Yes (+)	Yes (+)
June	No	No	Yes (-)
July	No	No	No
August	No	No	No
September	Yes (+)	Yes (+)	Yes (-)
October	Yes (-)	Yes (-)	Yes (-)
November	Yes (+)	Yes (+)	Yes (+)
December	No	No	No

Trend test to analyze the temporal dynamics of precipitation within the Ghis-Nekor plain

The presented innovative trend methodology was applied to different precipitation time series recorded at the Ghis-Nekor gauging station. An average precipitation time series was evaluated for the monthly time scale, and a trend analysis was performed by applying the ITA method. The results of the ITA approach were compared with those obtained by the Man-Kendall monotonic test applied to the original series. Each monthly value is represented by its estimated mean between the periods 1992 and 2020.

Figure 6 shows the results of the ITA method applied to the Ghis-Nekor station, reflecting the monthly precipitation trends between 1992 and 2020. Each scatter plot corresponds to a specific month, where the x-axis represents the precipitation values during the first half of the study period (1992–2005), and the y-axis represents the values for the second half (2006–2019). The orange diagonal line serves as the 1:1 reference line, indicating no change in precipitation between the two periods. The points above this line signify an increasing trend, while the points below indicate a decreasing trend in precipitation. The results highlight varying patterns across the months, with noticeable increases in some months (e.g., September, November, and February), while

others (e.g., July) exhibit limited or no significant trends. These findings provide a clear visualization of the temporal dynamics and monthly variability in precipitation within the Ghis-Nekor plain over the study period.

The ITA applied to the monthly precipitation data at Ghis-Nekor station provides a detailed interpretation of precipitation trends by categorizing the data into three classes: low (<20 mm), medium (20–40 mm), and high (>40 mm). This classification facilitates understanding of precipitation dynamics across months. The interpretation is as follows:

- January: An upward trend is observed for all categories (low, medium, high), indicating an increase in precipitation across all levels during the second half of the study period.
- February: Similar to January, there is an upward trend for all precipitation categories, reflecting consistent increases.
- March: A downward trend is observed across all categories (low, medium, high), suggesting a decrease in precipitation levels compared to the earlier period.
- April: All categories exhibit an upward trend, signifying a notable increase in precipitation.
- May: Precipitation shows an upward trend across all categories, indicating improvements in rainfall patterns for this month.
- June: For the low and medium categories, there is no trend, indicating stability in precipitation

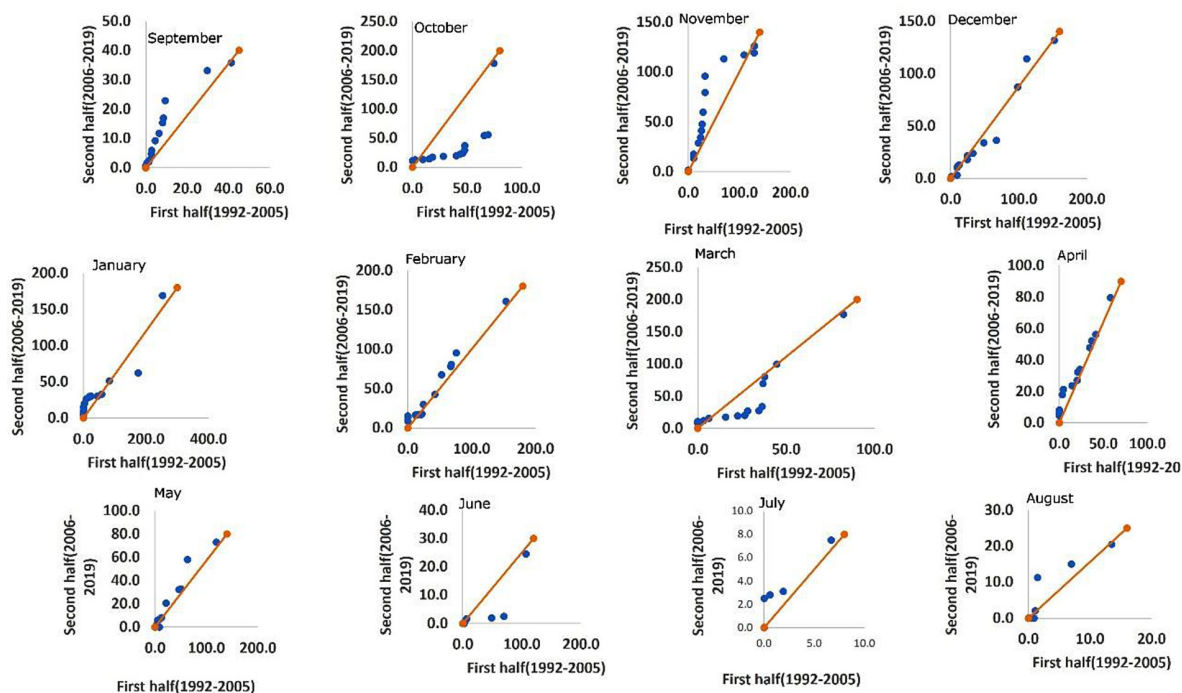


Figure 6. Result of the ITA test at the Ghis-Nekor aquifer

levels. However, for the high category, there is a slight downward trend, showing a reduction in heavy rainfall.

- July: There is no trend for any of the categories, suggesting no significant changes in precipitation.
- August: Similar to July, there is no trend observed across all categories.
- September: For the low and medium categories, there is an upward trend, indicating an increase in light and moderate precipitation. However, for the high category, a downward trend is observed, reflecting a decline in heavy precipitation.
- October: A downward trend is evident across all categories, suggesting a decrease in precipitation levels during this month.
- November: All categories (low, medium, high) show an upward trend, highlighting a consistent increase in precipitation.
- December: There is no trend observed for any of the categories, indicating stable precipitation conditions.

This analysis highlights seasonal variability in precipitation trends within the Ghis-Nekor plain. The months of January, February, April, May, and November exhibit consistent upward trends across all categories, which indicate positive changes in precipitation. In contrast, March and October show clear downward trends across all categories. For June, July, August, and December, trends are minimal or nonexistent, and reflect a stable or unchanged conditions. September displays a mixed behavior, with upward trends in light and moderate precipitation but a decline in heavy rainfall. These insights reveal a nuanced understanding of monthly precipitation dynamics and an overall declining trend in annual precipitation levels.

Figure 7 presents the annual ITA test results for the Ghis-Nekor plain. In this figure, most of the blue points are located below the reference line, which show a decreasing trend in annual precipitation across the two periods. The significant clustering of points in the lower and middle range (100–200 mm) reflects a reduction in precipitation intensity over time. The downward shift of the points away from the reference line further supports the overall negative trend. Only a few data points align with or slightly above the line, showing rare instances of stable or slightly increased precipitation. This result aligns with the broader findings of decreasing

annual precipitation trends in the Ghis-Nekor plain, which could have implications for water availability, agricultural productivity, and resource management in the studied area.

On the basis of the previous results of these tests, it is evident that the ITA method offers greater reliability compared to the Mann-Kendall method. The Mann-Kendall analysis indicates no significant trend, whereas the ITA method reveals significant trends across different precipitation categories. For instance, in January, the low precipitation category exhibits a decreasing trend, while the average precipitation category shows an increasing trend.

Analysis of satellite climate data

FLDAS model

Figure 8 presents the decomposition of the few land data assimilation (FLDAS) precipitation time series into three components: trend, seasonality, and residual. The trend highlights three distinct periods of variation: a decreasing trend from 2002 to 2005, an increasing trend from 2005 to 2010, and a stable to slightly decreasing trend from 2010 to 2018. The seasonality component reveals a clear annual cycle, showing consistent periodic fluctuations in precipitation patterns throughout the years. The residual (remainder) component captures the irregular variations that are not explained by the trend or seasonality, with small deviations around the baseline except for a noticeable increase in variability after 2016.

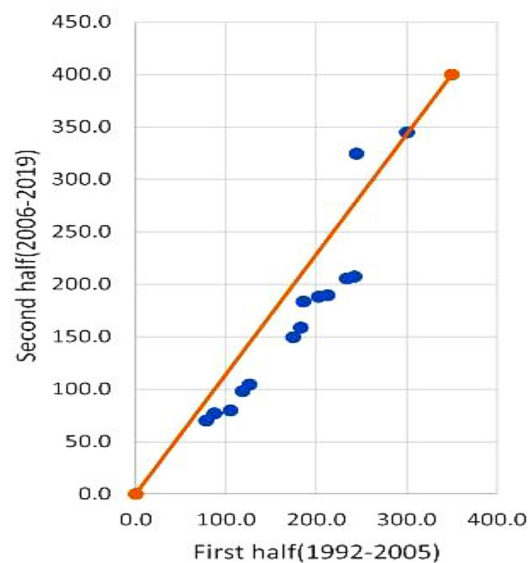


Figure 7. Annual ITA test results at the Ghis-Nekor plain level

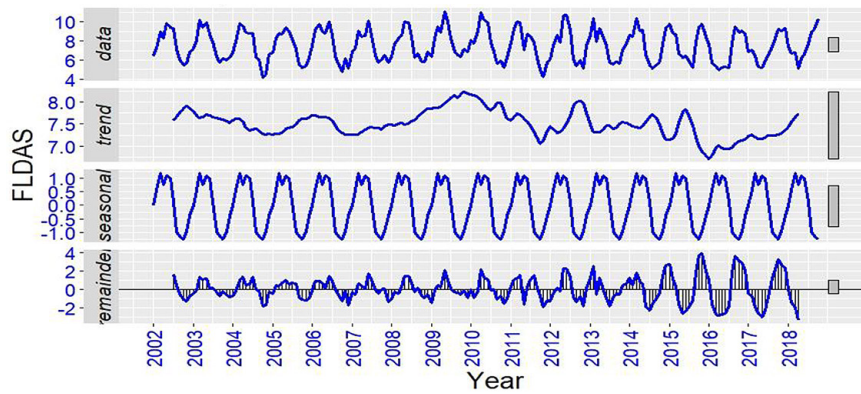


Figure 8. Chronological decomposition of precipitation from the FLDAS model

Overall, the decomposition effectively distinguishes the underlying structure of the FLDAS precipitation data, which emphasize both long-term trends, and recurring seasonal behavior within the Nekor basin.

IMERG model

Figure 9 displays the decomposition of the IMERG precipitation time series for the Ghis-Nekor water table into trend, seasonality, and residual components. The trend highlights three main phases: a decreasing trend from 2002 to 2011, a rising trend from 2011 to 2015, and a subsequent decline from 2015 to 2018, aligning with the reported long-term variability. The seasonal component shows a clear pattern of the alternating wet and dry seasons, which indicate a consistent seasonal cycle of rainfall in the Ghis-Nekor area.

Finally, the residual component captures irregular fluctuations not explained by the trend or seasonal patterns, with notable variability observed throughout the time series, particularly after 2007.

This decomposition effectively captures the annual cycles, long-term trends, and irregular variations in the IMERG precipitation over the study period.

Precipitation correlation

Correlation of time series between the models

Figure 10 illustrates the correlation between FLDAS, IMERG, and observed precipitation at the Ghis-Nekor aquifer by using a 12-month moving average. The IMERG (blue line) and measured precipitation (red line) demonstrate a strong correlation, following similar trends over time, although IMERG often shows higher amplitudes, indicating a slight overestimation of precipitation. The FLDAS data (green line), on the other hand, remains relatively stable and shows consistently lower values compared to the other series. The overall pattern highlights that satellite-derived precipitation data (IMERG and FLDAS) capture the general trend of measured precipitation, but IMERG provides higher variability and better alignment with

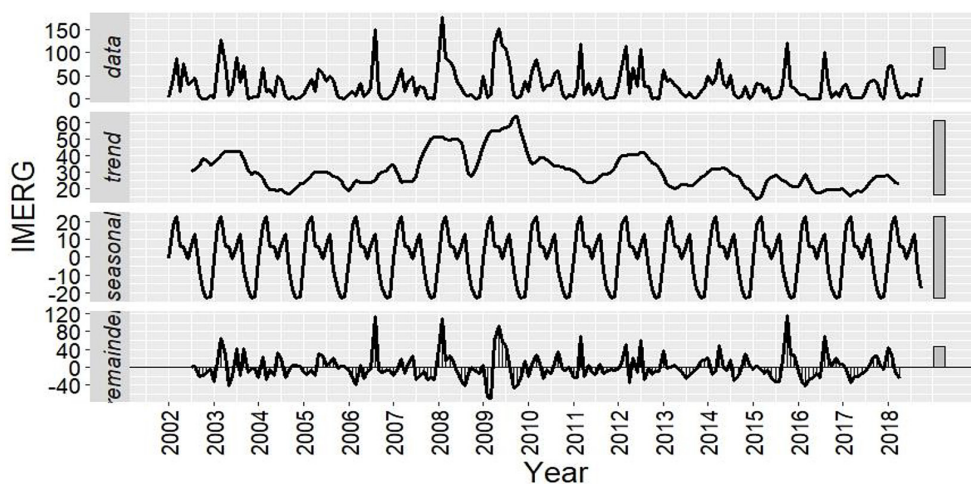


Figure 9. Chronological decomposition of precipitation from the IMERG model

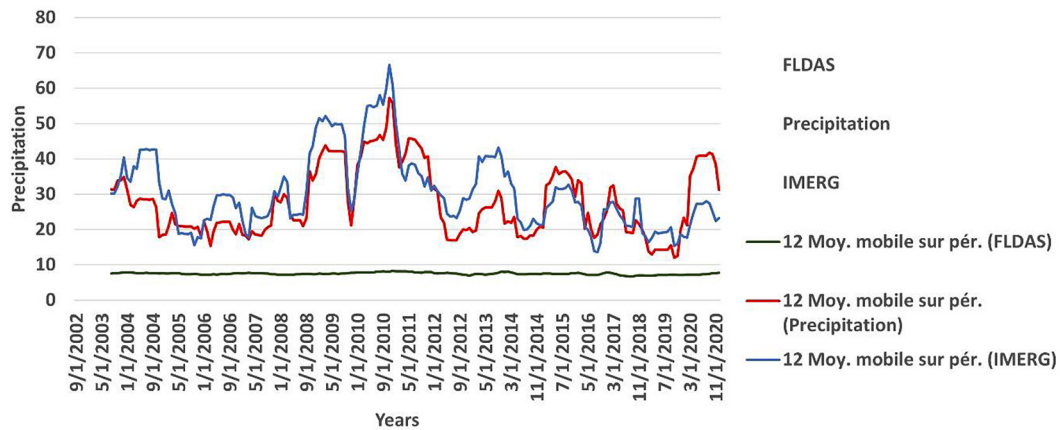


Figure 10. Correlation between the PM, FLDAS, and IMERG models

observed seasonal fluctuations. This comparison underscores the reliability of satellite products for monitoring precipitation trends while acknowledging their tendency to overestimate precipitation levels compared to ground observations.

Presentation of monthly average water storage anomalies derived from TWS_GRACE

The monthly mean TWS variations in sinusoidal form with many peaks in spring and summer and a general decline in winter. It highlighted the effect of summer precipitation and flash floods. The GRCTellus Land RL06 version of the Gravity recovery and climate data experiment (GRACE) as well as Gravity recovery and climate experiment (GRACE/FO) of these centers are available in two different solutions, namely, the spherical harmonic and the mascon (mass concentration blocks). Figure 11 displays TWS_GRACE-derived water storage anomalies for the Ghis-Nekor aquifer from 2002 to 2018. The trend highlights significant fluctuations in total water storage (TWS) anomalies

over the years. Initially, from 2002 to 2005, water storage shows a gradual increase with intermittent declines. Between 2008 and 2012, a notable peak phase occurs, indicating a period of higher water storage levels. However, post-2012, the water storage anomalies exhibit a consistent declining trend, with significant reductions observed from 2014 onward, reaching their lowest values by 2018. This pattern suggests that after a period of relative stability and gain, the Ghis-Nekor aquifer experienced sustained water loss, likely due to factors such as increased groundwater extraction, reduced recharge, or changing climatic conditions. The overall trajectory underscores a concerning decline in groundwater resources over the analyzed period.

Table 4 presents the Mann-Kendall test results for TWS_GRACE over the three phases (2002–2023) at the Ghis-Nekor aquifer. The results reveal significant trends in terrestrial water storage (TWS) anomalies. In Phase 1, the p-value is 3.452e-07, indicating a statistically significant decreasing trend, with a Z MK value of -5.0969 and a Sen slope of -0.0701 cm/year, which reflect

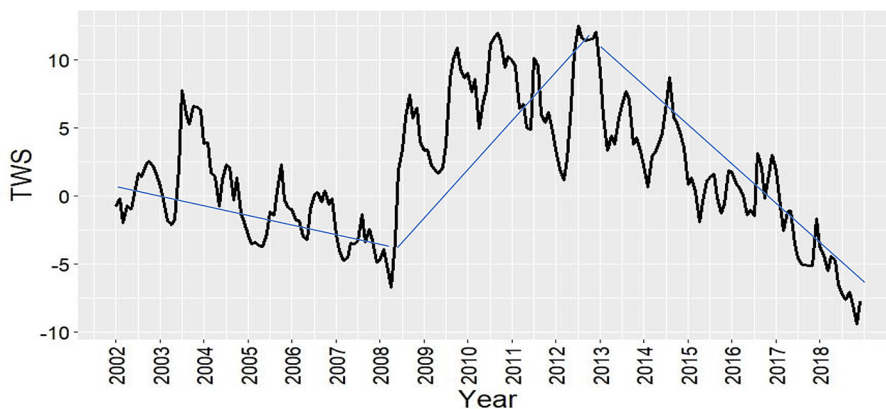


Figure 11. TWS_GRACE derived water storage anomalies at the Ghis-Nekor aquifer

Table 4. Mann-Kendall test for the three phases of TWS_GRACE

Phase	The Mann-Kendall trend test				
	p-value	H 0: No trend	Z MK	Sen slope (cm/year)	Trend direction
Phase 1	3.452e-07	No	-5.0969	-0.0700884	Drop
Phase 2	1.495e-05	No	4.3295	0.1286588	High
Phase 3	< 2.2e-16	No	-9.5399	-0.2067817	Drop

a drop in water storage. Phase 2, shows the intermediate period, indicating a positive trend with a p-value of 1.495e-05, a Z MK value of 4.3295, and a Sen slope of 0.1287 cm/year, shows a significant increase in water storage. However, in Phase 3, the results highlight a pronounced decline, with a p-value of <2.2e-16, a Z MK value of -9.5399, and a steep Sen slope of -0.2068 cm/year, confirming a strong drop in TWS. These findings underscore alternating phases of water gain and loss, with an overall trend of declining water storage, particularly during the third phase, suggesting increasing stress on groundwater resources in the Ghis-Nekor aquifer.

Estimation of changes in groundwater storage within the Ghis-Nekor aquifer level

Figure 12 presents the calculation of groundwater storage (GWS) at the Ghis-Nekor plain using the relationship $GWS = TWS - SM$, where SM represents soil moisture, and TWS is total terrestrial water storage.

- Panel A (TWS): The black line shows the total terrestrial water storage anomalies from 2002 to 2018. TWS exhibits significant fluctuations with a peak around 2010–2012, followed by a notable decline through 2018, reflecting a sustained reduction in total water storage.
- Panel C (SM): The blue line displays soil moisture variations, which demonstrate a seasonal cycle with consistent annual peaks and troughs throughout the study period. This indicates regular variability in soil moisture, likely driven by precipitation and evapotranspiration.
- Panel B (GWS): The red line represents groundwater storage, derived as the difference between TWS and SM. GWS reveals an overall declining trend, with notable reductions after 2012, indicating increasing groundwater depletion over time. The drop in GWS is more pronounced compared to fluctuations in soil moisture, highlighting the influence of groundwater extraction and reduced recharge rates.

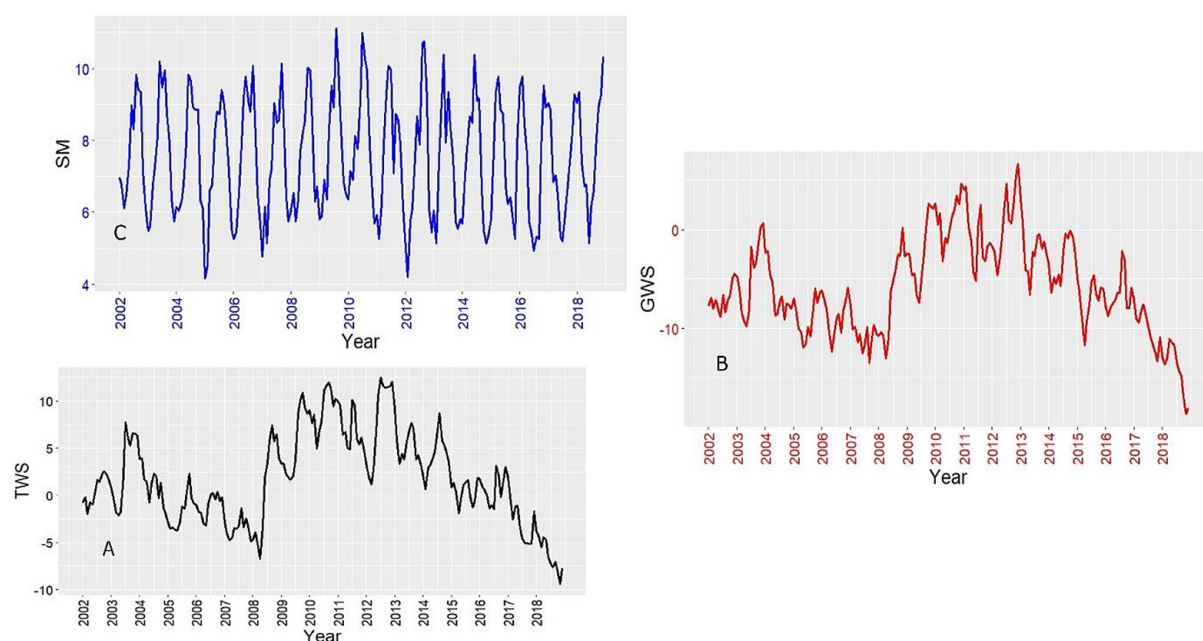


Figure 12. Calculation of GWS using soil moisture (C), TWS (A), and GWS (B)

In summary, while soil moisture (SM) remains relatively stable seasonally, the decline in TWS and the resulting GWS trends underscore significant groundwater loss, particularly in recent years, pointing to unsustainable water resource management in the Ghis-Nekor plain .

The Mann-Kendall test results for the four phases of groundwater storage (GWS) at the Ghis-Nekor aquifer reveal significant trends over the study period (Table 5).

- In Phase 1, the p-value is 1.872e-06, indicating a statistically significant decreasing trend. The Z MK value of -4.7667 and a Sen slope of -0.0631 cm/year reflect a noticeable drop in groundwater storage during this phase.
- Phase 2 shows a significant positive trend, with a p-value of 1.322e-06, a Z MK value of 4.8365, and a Sen slope of 0.1503 cm/year, indicating a high increase in groundwater storage.
- In Phase 3, the p-value is extremely small (< 2.2e-16), highlighting a strong decreasing trend. The Z MK value of -9.1705 and a steep Sen slope of -0.2025 cm/year confirm a substantial drop in GWS, representing the most severe decline across all phases.

Overall, the analysis reveals alternating periods of water gain and loss, with the final phase showing a critical and accelerated depletion of groundwater resources in the Ghis-Nekor aquifer, suggests an increasing water stress, and the need for improved groundwater management strategies.

Correlation between GWS and TWS

Figure 13 and Table 6 illustrate the relationship between terrestrial water storage (TWS) and groundwater storage (GWS) at the Nekor aquifer from 2002 to 2019. Both series exhibit a strong correlation, as the trends and fluctuations closely align throughout the time period. From 2002 to 2010, both TWS and GWS display alternating increases and decreases, reaching their peak around 2010–2012. Post-2012, there is a consistent declining trend in both TWS and GWS, with a particularly sharp decrease observed after 2017, highlighting significant water loss. This decline reflects growing groundwater depletion, likely due to increased extraction and reduced recharge. The strong alignment between the two series confirms that variations in TWS largely drive changes in GWS, emphasizing the

Table 5. Mann-Kendall test for the three phases of the GWS at the level of the Ghis-Nekor aquifer

Phase	The Mann-Kendall trend test				
	p-value	H 0: No trend	Z MK	Sen slope (cm/year)	Trend direction
Phase 1	1.872e-06	No	-4.7667	-0.06309078	Drop
Phase 2	1.322e-06	No	4.8365	0.1502888	High
Phase 3	< 2.2e-16	No	-9.1705	-0.2024977	Drop

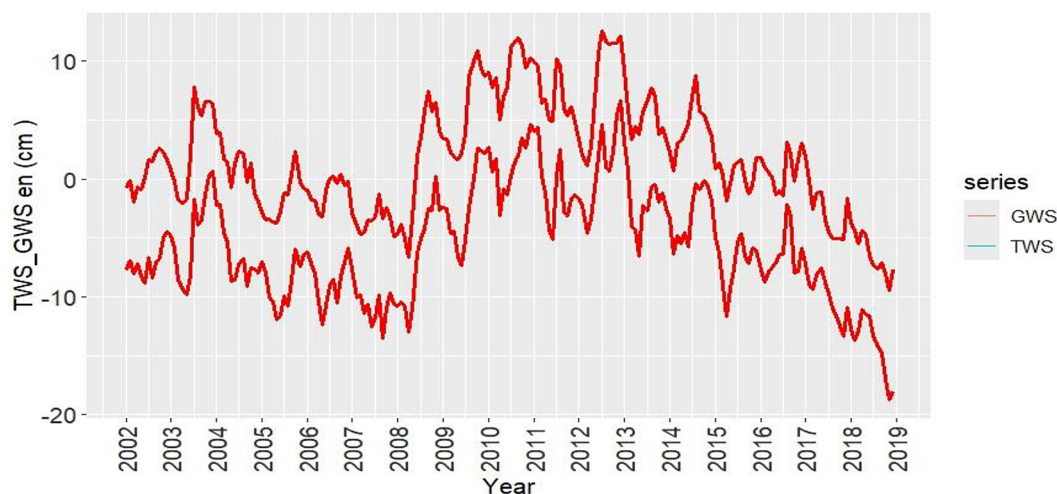


Figure 13. Correlation between GWS and TWS of the Ghis-Nekor aquifer

Table 7. Comparison between TWS and GWS at the level of the Ghis-Nekor plain

Phase	The Mann-Kendall trend test		
	TWS	GWS	Trend direction
	Sen slope (cm·a ⁻¹)	Sen slope (cm·a ⁻¹)	
Phase 1	-0.070	-0.063	Drop
Phase 2	0.128	0.150	Increase
Phase 3	-0.206	-0.202	Drop

interdependence between terrestrial and ground-water storage within the Nekor aquifer system.

Impact of drought on groundwater

Figure 14 highlights the relationship between precipitation (PM) and terrestrial water storage (TWS) anomalies over the period of 2002–2020, with 12-month moving averages for both variables. The blue line represents precipitation, while the orange line shows TWS anomalies. A strong correlation is observed between the two parameters, indicating that variations in precipitation significantly influence TWS trends. Peaks in precipitation, notably in 2004, 2006, 2009, 2010, and 2021, correspond with noticeable increases in TWS anomalies, demonstrating the direct impact of extreme precipitation events on terrestrial water storage. Conversely, drought periods, such as 2006, 2012, 2014, and 2019, are marked by sharp decreases in TWS, reflecting reduced water availability due to insufficient precipitation. Over the long term, TWS anomalies exhibit a gradual decline, suggesting the cumulative impact of droughts and reduced precipitation on terrestrial water storage. This analysis underscores the

sensitivity of TWS to precipitation variability and highlights the significant role of climate-related changes, such as droughts, in influencing the water storage dynamics in the study area.

Dynamic of precipitation and drought phases

Vulnerability of the aquifer to drought in the studied area

Figure 15 illustrates the standardized precipitation index (SPI) for the Ghis-Nekor plain from 1992 to 2020, showing the variability of wet and dry phases over the period. The SPI values fluctuate between positive (indicating wet conditions) and negative (indicating dry conditions), with varying magnitudes that classify the severity of droughts and wet periods into six categories: extremely dry, moderately dry, very dry, moderately humid, very humid, and extremely humid.

From the figure and the provided analysis, extremely dry years are observed in 1992, 1994, 1997, 1998, 2002, 2003, 2007, 2008, 2010, 2014, and 2020, characterized by significant negative SPI values. In contrast, moderately dry years include 2000, 2006, 2008, 2010, 2012, 2015, 2016, 2017, 2018, and 2019, showing smaller negative

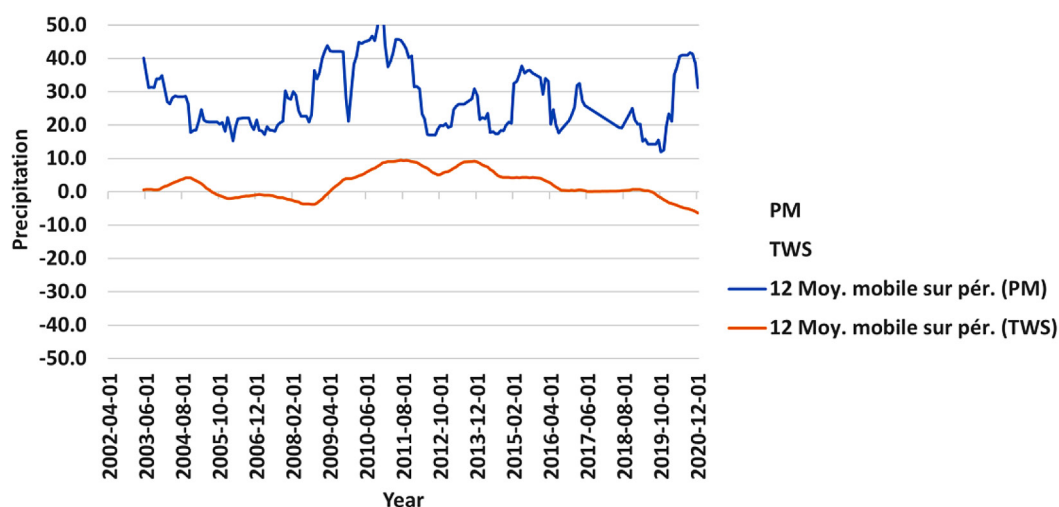


Figure 14. Correlation between PM, TWS at the Ghis-Nekor water table level

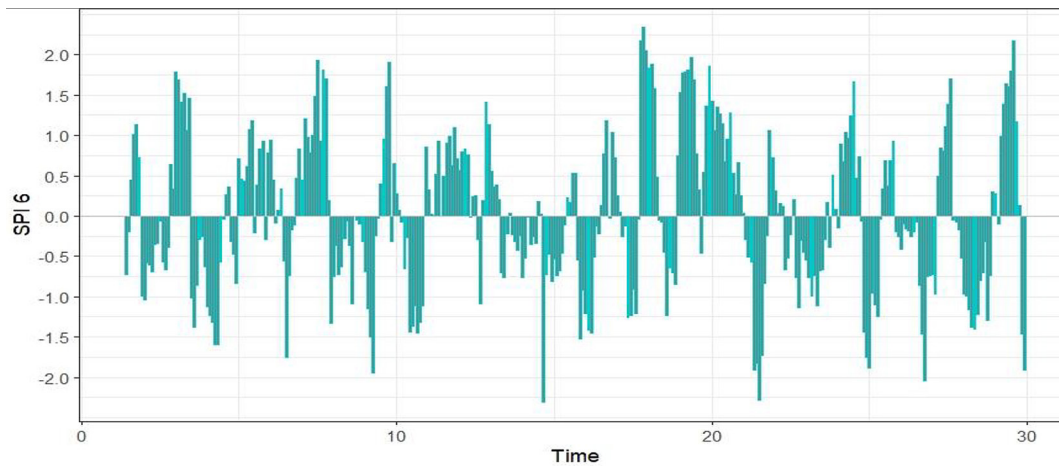


Figure 15. Variation of drought index ISP during 1992_2021

SPI values. Additionally, very dry years such as 1994, 1995, and 2000 reflect more severe drought conditions. Wet phases are also evident, marked by positive SPI values, indicating periods of moderately to extremely humid conditions.

The figure clearly highlights a dominance of dry phases interspersed with wet periods, reflecting the vulnerability of the aquifer to drought. The occurrence of frequent and extreme drought years, particularly in the last two decades, underscores the increasing climate variability in the region and its impact on water resources in the Ghis-Nekor plain.

Effect of drought on water storage within the Ghis-Nekor aquifer

Figure 16 illustrates the correlation between monthly precipitation (PM), terrestrial water storage (TWS), and groundwater storage (GWS) at the Ghis-Nekor water table level over the study

period (2002–2020). The blue line represents the 12-month moving average of precipitation, the red line shows the 30-month moving average of TWS, and the yellow line represents the 7-month moving average of GWS. A clear negative trend in groundwater storage (GWS) is observed, reflecting a continuous decline in groundwater levels. TWS, represented with a linear trend, also shows a downward trajectory, indicating overall water mass loss in the watershed (Meng et al., 2019).

Figure 16 highlights a strong correlation between precipitation, TWS, and GWS, showing that fluctuations in rainfall directly impact terrestrial and groundwater storage. Notably, periods of reduced precipitation correspond to sharp declines in both TWS and GWS, confirming the detrimental effects of climate variability and drought on the water balance. This analysis underscores the utility of GRACE satellite data for monitoring hydrological changes and supporting

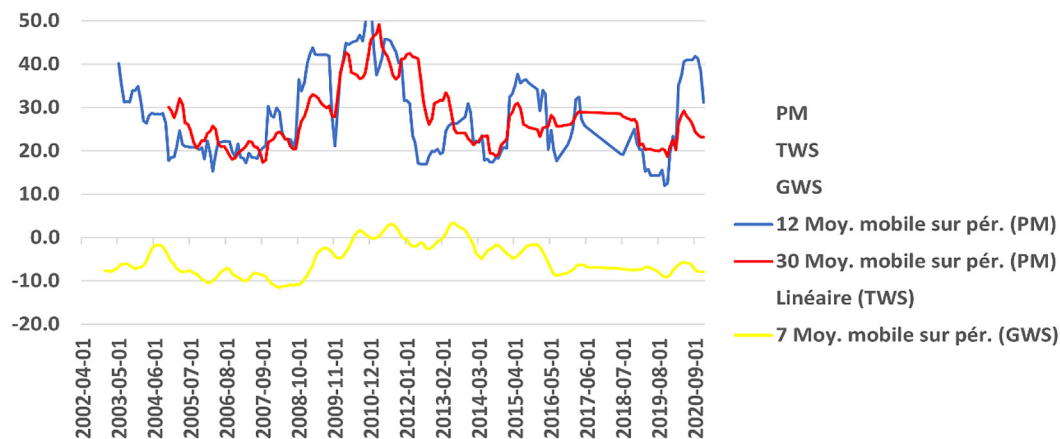


Figure 16. The correlation between measured precipitation, terrestrial water storage, and groundwater storage in the Ghis-Nekor aquifer

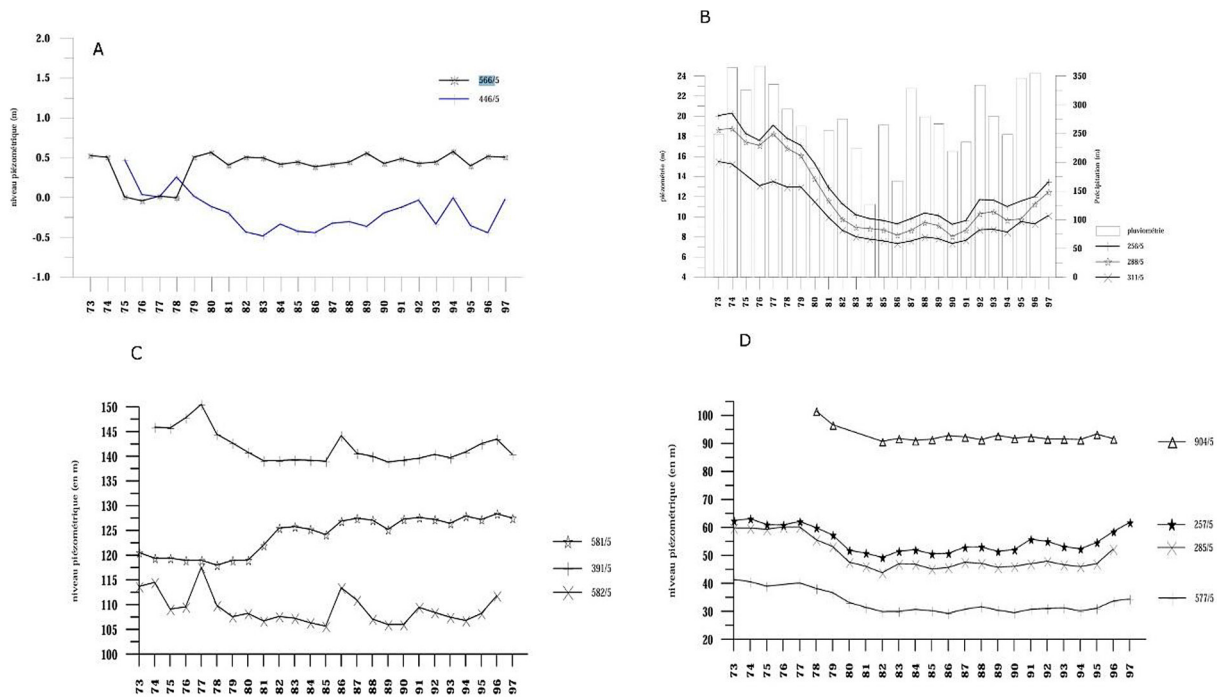


Figure 18. Fluctuation of piezometric levels in the Ghis-Nekor plain aquifer

from the early 1970s until the late 1980s, with lower precipitation values during this period correlating with reduced groundwater levels. A slight recovery is observed toward the late 1990s, which align with increased precipitation.

- Graph C: The graph illustrates the piezometric levels for three piezometers (581/5, 391/5, and 582/5) over time. All three series show a general downward trend with periodic fluctuations. Notably, piezometer 581/5 starts at a higher level and declines more rapidly compared to the others, suggesting significant water extraction in that region.
- Graph D: This graph focuses on four piezometers (904/5, 251/5, 285/5, and 571/5), highlighting persistent declines in piezometric levels over time. The levels remain relatively stable for 904/5, while piezometers like 285/5 and 571/5 show pronounced declines, particularly in the mid-1980s, reflecting the areas of significant groundwater stress.

CONCLUSIONS

In conclusion, the analysis of precipitation intensity and water storage dynamics in the Ghis-Nekor plain reveals significant temporal and spatial trends that highlight the vulnerability of the area to climate variability and water scarcity. The

scatter plot analysis indicates clear monthly variations in precipitation patterns, with some months showing consistent upward trends, while others, such as July and October, exhibit a decline or no significant change. The innovative trend analysis method provides a more detailed and reliable insight into these trends, revealing that precipitation has generally decreased over the study period, especially during the second half of the analysis, with certain months, such as January, February, and November, displaying notable increases.

The decomposition of satellite-derived precipitation data (FLDAS and IMERG models) further supports the findings, emphasizing the cyclical nature of precipitation and the variability driven by climate factors. The analysis of terrestrial water storage and groundwater storage also highlights a concerning decline in water resources, with the Ghis-Nekor aquifer showing significant water loss, particularly post-2012. The correlation between precipitation, TWS, and GWS indicates a strong interdependence, with reduced precipitation directly leading to declining water storage levels. Moreover, the impact of drought on groundwater resources is evident, as periods of reduced precipitation align with sharp declines in water storage and increased water stress.

These findings underscore the urgent need for improved water resource management and strategic planning, particularly in the face of increasing

climate variability and frequent droughts. The integration of satellite data, such as GRACE and the analysis of piezometric levels, provides a valuable tool for monitoring hydrological changes and supporting sustainable water management in the Ghis-Nekor aquifer. Ultimately, addressing the challenges posed by decreasing water availability will require a combination of effective resource management strategies, climate adaptation measures, and careful monitoring of both terrestrial and groundwater storage trends.

REFERENCES

- Alifujiang, Y., Abuduwaili, J., & Abliz, A. 2023. Precipitation trend identification with a modified innovative trend analysis technique over Lake Issyk-Kul, Kyrgyzstan. *Journal of Water and Climate Change*, 14(6), 1798-1815. <https://doi.org/10.2166/wcc.2023.413>.
- Amraoui, M., Bouabidi, L., El Amrani, M., Ouakhir, H., Dudic, B., Lukić, T., & Spalevic, V. 2024. Land use dynamics and soil conservation strategies in the El Kssiba Region, Atlas Mountains of Morocco. *Agriculture and Forestry*, 70(3), 7-27. <https://doi.org/10.17707/AgricultForest.70.3.01>
- Amraoui, M., Mijanovic, D., El Amrani, M., Kader, S. and Ouakhir, H. 2023. Agriculture and economic development of the Ait Werra tribe during the French colonialism period and its local characteristics (1912- 1956) within the middle atlas region of Morocco. *Agriculture and Forestry*, 69 (4): 91-112. [doi:10.17707/AgricultForest.69.4.07](https://doi.org/10.17707/AgricultForest.69.4.07)
- Chakir, M., Ghadbane, O., Ouakhir, H., Ghachi, M.E. 2024. Flow Duration Curve a Tool for Assessing the Intensity and Seasonal Patterns of Low-Flow Periods: Case Study of Tassaout River Basin Within the Upstream of Moulay Youssef Dam (1978–2016) (Morocco). In: Azrour, M., Mabrouki, J., Guezzaz, A. (eds) *Sustainable and Green Technologies for Water and Environmental Management*. World Sustainability Series. Springer, Cham. https://doi.org/10.1007/978-3-031-52419-6_11
- Chakir, M., Ghadbane, O., Ouakhir, H., & El Ghachi, M. 2023. Extraction et analyse des phases de tarissement: application dans le bassin versant de l’oued Tassaout (amont du Barrage Moulay Youssef), Haut Atlas Central, Maroc (1978-2016). *Afrique SCIENCE*, 22(2), 129-141. X, <http://www.afrique-science.net>
- Chen, H., Zhang, W., Nie, N., & Guo, Y. 2019. Long-term groundwater storage variations estimated in the Songhua River Basin by using GRACE products, land surface models, and in-situ observations. *Science of the total environment*, 649, 372-387. doi.org/10.1016/j.scitotenv.2018.08.352.
- Chen, J., Cazenave, A., Dahle, C., Llovel, W., Pagnet, I., Pfeffer, J., & Moreira, L. 2022. Applications and challenges of GRACE and GRACE follow-on satellite gravimetry. *Surveys in Geophysics*, 43(1), 305-345. <https://link.springer.com/article/10.1007/s10712-021-09685-x>
- Cheng, Y., Arapin, A., Zhang, Z., Zhang, Q., Li, H., Feamster, N., & Jiang, J. 2022. Grace: Loss-resilient real-time video communication using data-scalable autoencoder. *arXiv preprint arXiv:2210.16639*. <https://doi.org/10.48550/arXiv.2210.16639>
- Drouiche, A., Nezzal, F., & Djema, M. 2019. Interannual variability of precipitation in the Mitidja plain in northern Algeria. [DOI: 10.7202/1065205ar](https://doi.org/10.7202/1065205ar)
- Ennaji N, Ouakhir H, Halouan S, Abahrour M. 2022. Assessment of soil erosion rate using the EPM model: case of Ouaoumana Assessment of soil erosion rate using the EPM model : case of Ouaoumana basin , Middle Atlas , Morocco . [DOI 10.1088/1755-1315/1090/1/012004](https://doi.org/10.1088/1755-1315/1090/1/012004) .
- Ennaji, N., Ouakhir, H., Abahrour, M., Spalevic, V., & Dudic, B. 2024. Impact of watershed management practices on vegetation, land use changes, and soil erosion in River Basins of the Atlas, Morocco. *Notulae Botanicae Horti Agrobotanici Cluj-Napoca*, 52(1), 1–12. <https://doi.org/10.15835/nbha52113567> .
- Güçlü, Y. S. 2018. Multiple Şen-innovative trend analyses and partial Mann-Kendall test. *Journal of Hydrology*, 566, 685-704. <https://doi.org/10.1016/j.jhydrol.2018.09.034>.
- Hamdi., M. 2023a. Response of an aquifer system to climate change and anthropogenic stress: contribution of numerical modeling and satellite gravimetry. *Thesis defend at University of Sherbrooke Faculty of Letters and Human Sciences, Department of Applied Geomatics*. [DOI: 10.13140/RG.2.2.25391.51361](https://doi.org/10.13140/RG.2.2.25391.51361)
- Hamdi., M. 2023b. Response of an aquifer system to climate change and anthropogenic stress: contribution of numerical modeling and satellite gravimetry. *Thesis defend at University of Sherbrooke Faculty of Letters and Human Sciences, Department of Applied Geomatics*. [DOI: 10.13140/RG.2.2.25391.51361](https://doi.org/10.13140/RG.2.2.25391.51361).
- Kendall, M. G. 1948. Rank correlation methods. <https://psycnet.apa.org/record/1948-15040-000>.
- Klemme, H. D. 1958. Regional geology of circum-Mediterranean region. *AAPG Bulletin*, 42(3), 477-512. <https://archives.datapages.com/data/bulletns/195760/data/pg/0042/0003/0450/0477.htm>.
- Mann, H. B. 1945. Nonparametric tests against trend. *Econometrica: Journal of the econometric society*, 245-259. <https://doi.org/10.2307/1907187> .
- Meng, C., Zhang, H., Wang, Y., Wang, Y., Li, J., & Li, M. 2019. Contribution analysis of the spatial-temporal changes in streamflow in a typical

- elevation transitional watershed of southwest china over the past six decades. *Forests*, 10(6), 495. <https://www.mdpi.com/1999-4907/10/6/495>
19. Nouayti, N., Cherif, E. K., Algarra, M., Pola, M. L., Fernández, S., Nouayti, A., ... & Rodero, A. 2022. Determination of physicochemical water quality of the ghis-nekor aquifer (Al Hoceima, Morocco) using hydrochemistry, multiple isotopic tracers, and the geographical information system (GIS). *Water*, 14(4), 606. <https://doi.org/10.3390/w14040606>
20. Ouakhir, H., & El Ghachi, M. 2023. Temporal Dynamic of Soil Erosion and Rainfall Erosivity Within Srou River Basin (Middle Atlas / Morocco). *American Journal of Mechanics and Applications*, 11(1), 1–5. <https://doi.org/10.11648/j.ajma.20231101.11>
21. Ouakhir, H., Ennaji, N., Spalevic, V., Gomih, M., Ghadbane, O., Chakir, M., & El Ghachi, M. 2023. Changes in river bank morphology in a small meander of El Abid River, Atlas Mountains, Morocco. *Poljoprivreda i Sumarstvo*, 69(3), 199-209. DOI: [10.17707/AgricultForest.69.3.14](https://doi.org/10.17707/AgricultForest.69.3.14)
22. Pascal, C. 2022. Cartographie multi-échelle des ressources en eau sur les régions irriguées : une approche par télédétection multi-capteurs. (*Doctoral dissertation, Université Paul Sabatier-Toulouse III*). <https://theses.hal.science/tel-04139330>.
23. Salhi, A., Martin-Vide, J., Benhamrouche, A., Benabdelouahab, S., Himi, M., Benabdelouahab, T., & Casas Ponsati, A. 2019. Rainfall distribution and trends of the daily precipitation concentration index in northern Morocco: a need for an adaptive environmental policy. *SN Applied Sciences*, 1(3), 277. <https://link.springer.com/article/10.1007/s42452-019-0290-1> .
24. Zheng, Y., Yang, M., & Liu, H. 2024. Coastal groundwater dynamics with a focus on wave effects. *Earth-Science Reviews*, 104869. <https://www.sciencedirect.com/science/article/pii/S001282522400196X>